Radioactively Powered Light Curves

Anirudh Patel
Department of Physics & Columbia Astrophysics Laboratory, Columbia University
anirudh.p@columbia.edu

August 4, 2025

Abstract

Notes for the summer school on astrophysical transients at the Center for Computational Astrophysics, Flatiron Institute (July 28 - August 8, 2025). There is an accompanying Python notebook that can be found on Github.

1 Motivation

Thermonuclear SNe are powered by energy released during rapid nuclear burning of light nuclei (^{12}C, ^{16}O) into heavier and more tightly bound nuclei (^{56}Ni and other iron group nuclei). With this information we can estimate the typical energy scale of Type Ia SNe, which are triggered by runaway thermonuclear fusion in white dwarfs. Let's assume we have a $1M_\odot$ white dwarf made entirely of ^{16}O, and that all the ^{16}O is burned to ^{56}Ni. The binding energies of ^{16}O and ^{56}Ni are ≈ 8 MeV nucleon^{-1} and ≈ 8.6 MeV nucleon^{-1}, respectively, and so $\Delta E = 0.6$ MeV nucleon^{-1}. There are $N \approx 1M_\odot/m_p \sim 10^{57}$ nucleons in the White Dwarf, so the total energy released in the fusion process is $N\Delta E \approx 6 \times 10^{56}$ MeV $\approx 10^{51}$ erg. The ^{56}Ni, along with other iron-group nuclei, synthesized in the explosion are unstable to radioactive decay and provide the sustained energy source powering the SNe light curve. Here we discuss approximate analytical models for these light curves. We consider SNe Ia light curves as an example, but the model can be easily generalized to other radioactively (e.g., r-process) powered transients.

2 One-zone light curve model

We will first model the ejecta as a spherical, uniform-density cloud of mass M and constant opacity κ expanding homologously ($r(t) \simeq vt$). The internal energy $E_{\rm int}(t)$ evolves according to the first law of thermodynamics,

$$\frac{dE_{\rm int}}{dt} = \dot{Q} - P\frac{dV}{dt} - L, \tag{1}$$

where $\dot{Q}(t)$ is the power source term (e.g., for radioactivity), the second term accounts for adiabatic losses, and $L(t)$ is the radiated luminosity.[1] For radiation dominated ejecta, $P = \frac{E}{3V}$ where the volume evolves as $V(t) = \frac{4}{3}\pi(vt)^3$ under homologous expansion. Under the diffusion approximation, $L(t) \simeq E_{\rm int}/t_{\rm diff}$, where $t_{\rm diff}(t) = t_{\rm pk}^2/t$ and $t_{\rm pk} = \sqrt{\kappa M/4\pi c v}$ is approximately the peak time of the transient. We can then rewrite Eq. 1 as an ODE for the luminosity,

$$\frac{d}{dt}(Lt_{\rm diff}) = \dot{Q} - L\frac{t_{\rm diff}}{t} - L. \tag{2}$$

with the general solution,

$$L(t) = \frac{2}{t_{\rm pk}^2}\exp\left(-\frac{t^2}{t_{\rm pk}^2}\right)\int_0^t t'\dot{Q}(t')\exp\left(\frac{t'^2}{t_{\rm pk}^2}\right)dt'. \tag{3}$$

[1] To satisfy energy conservation one must allow for acceleration of the ejecta by coupling Eq (1) with another differential equation for kinetic energy $dE_{\rm kin}/dt = P(dV/dt)$, however, the constant velocity assumption will be good enough for our purposes where the energy dumped into the system from radioactive heating is small compared to the initial kinetic energy of the ejecta.

From Eq. (2), it is evident that $L = \dot{Q}$ when $dL/dt = 0$. In other words, the radiated luminosity at peak time is equal to the radioactive heating rate. This is known as "Arnett's rule" (Arnett, 1980). Note, that this approximate one-zone solution can be used for *any* transient under the assumptions laid out above; one just needs to specify the parameters M, v, κ, and $\dot{Q}$.

2.1 Applied to Type Ia Supernovae

As a first exercise, let's apply the model to the case of SNe Ia. For the fiducial case, we will take $M = 1.4 M_\odot$, $v = \sqrt{2E_{\rm kin}/M} \sim 10^4$ km s^{-1}, and $\kappa \approx 0.2$ cm^2 g^{-1} (for a mixture of alpha- and iron-group elements), where we have assumed $E_{\rm kin} = 10^{51}$ erg. The specific radioactive energy generation rate from the ^{56}Ni $\rightarrow ^{56}$Co $\rightarrow ^{56}$Fe decay chain is,

$$\dot{q}(t) = (\epsilon_{\rm Ni} - \epsilon_{\rm Co}) e^{-t/t_{\rm Ni}} + \epsilon_{\rm Co} e^{-t/t_{\rm Co}}, \tag{4}$$

where $\epsilon_{\rm Ni} = 3.9 \times 10^{10}$ erg s^{-1} g^{-1}, $\epsilon_{\rm Co} = 6.8 \times 10^9$ erg s^{-1} g^{-1}, $t_{\rm Ni} = 8.8$ days, and $t_{\rm Co} = 111.3$ days. The total heating function becomes $\dot{Q}(t) = M_{\rm Ni} \dot{q}(t)$ where $M_{\rm Ni}$ is the mass of ^{56}Ni synthesized in the explosion. We will take $M_{\rm Ni} = 0.7 M_\odot$. The resulting light curve is presented in Fig. 1. You will notice the light curve converges to the heating rate from the ^{56}Ni decay chain after peak, as predicted from Arnett's rule. The luminosity-scale and time-scale also align well with SNe Ia observations.

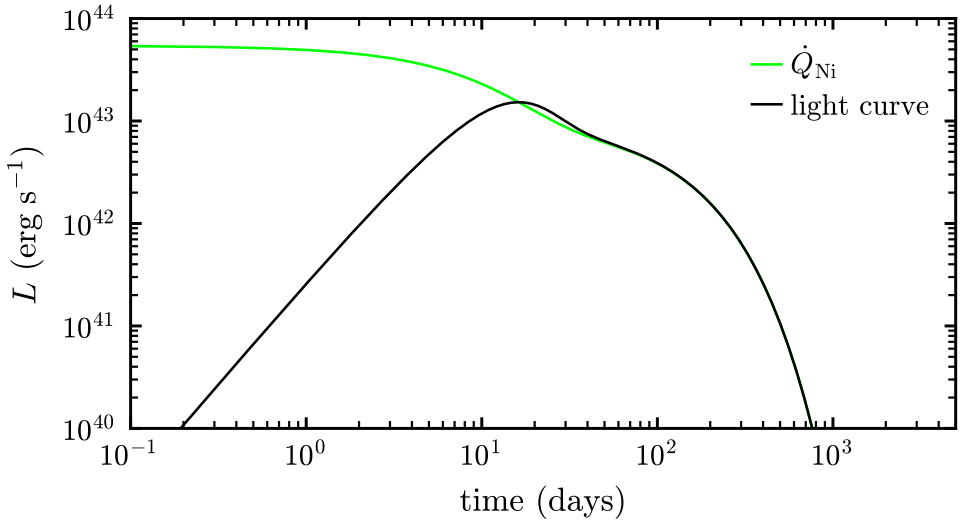

Figure 1: One-zone light curve for fiducial model parameters, $M = 1.4 M_\odot$, $M_{\rm Ni} = 0.7 M_\odot$, $\bar{v} = 10000$ km s^{-1}, and $\kappa = 0.2$ cm^2 g^{-1}.

3 Multi-zone light curve model

We can now extend our one-zone solution to a multi-zone light curve model, which allows for more realistic features such as radially dependent radioactive mass distribution, opacity, and velocity profiles for the ejecta - rather than the spatially uniform values required in a one-zone approach.

3.1 Setting up the ejecta model

It is convenient to work in Lagrangian mass coordinate $m \in [0, M]$, such that $m = 0$ corresponds to the outer-most layer at the surface of the ejecta while $m = M$ corresponds the inner-most layer at the center of the ejecta. We can assign a homologous velocity profile to the ejecta,

$$v(m) = \frac{\beta - 1}{\beta} \bar{v} \left(\frac{m}{M} \right)^{-1/\beta}, \tag{5}$$

where $\bar{v}$ is the average velocity and $\beta > 1$.[2] An example velocity profile for $\bar{v} = 10000$ km s^{-1} with $\beta = 5$ is shown in Fig 2.

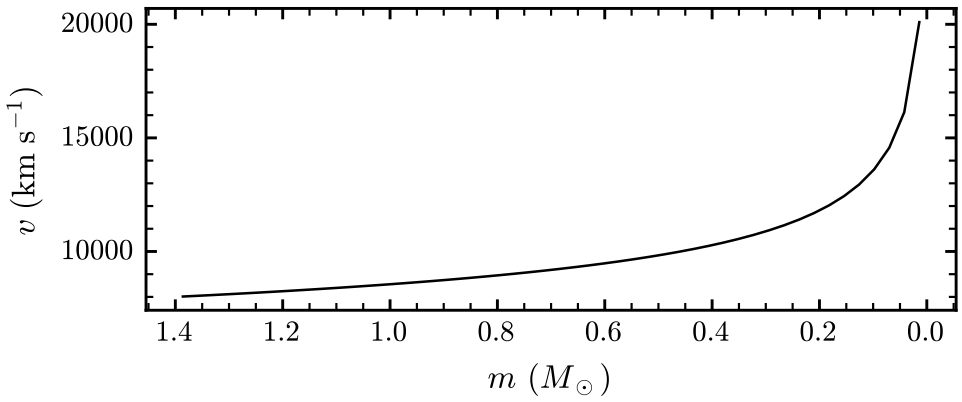

Figure 2:

Now we consider the distribution of radioactive material through the ejecta (e.g., ^{56}Ni). Again, we can treat the total mass of radioactive products synthesized in the explosion as a free parameter $M_{\rm rad}$. Lacking a self-consistent hydrodynamical explosion model, we will artificially mix the radioactive material from the inner ejecta layers (where we are assuming it is synthesized) into the outer ejecta layers. We adopt the mass distribution function from Patel et al. (2024),

$$X_{\rm rad}(m) = \mathcal{C}\left[\tanh\left(\frac{f_{\rm mix}M - M + m)}{0.2 f_{\rm mix} M}\right) + 1\right], \tag{6}$$

where the free parameter $f_{\rm mix}$ determines how far towards the surface the radioactive products are mixed. The constant $\mathcal{C}$ can be found by normalizing $M_{\rm rad} = \int X_{\rm rad} dm$. For an ejecta mass $M = 1.4 M_\odot$, ^{56}Ni mass $M_{\rm Ni} = 0.7 M_\odot$, and $f_{\rm mix} = 0.5$ (corresponding to nickel mixed out to mass coordinate $f_{\rm mix} M \approx 0.7 M_\odot$), we get the mass fraction profile in the bottom panel of Fig. 3. The shape of this profile shows good agreement with results obtained from 1D hydrodynamical simulations using more sophisticated mixing schemes (e.g., Woosley et al. 2007; Morozova et al. 2015).

The final ingredient we need is the opacity. The opacity structure may vary significantly for different systems depending on the ejecta composition and distribution, but a simple general form can be applied for (hydrogen-poor) supernovae,

$$\kappa(m) = \kappa_0 + \kappa_1 X_{\rm rad}(m), \tag{7}$$

where κ_0 corresponds to the continuum opacity of the outer ejecta and κ_1 corresponds to the opacity of the radioactive material. The radioactive material consists of heavier metals (iron group or heavier) contributing greater opacity than the outer ejecta, which is depleted in heavy metals. For example, in SNe Ia, we may take $\kappa_0 \approx 0.1$ cm^2 g^{-1} for alpha-group elements and $\kappa_1 \approx 0.3$ cm^2 g^{-1} for ^{56}Ni and other iron-group elements. The top panel of Fig. 3 shows the opacity profile corresponding to the nickel mass fraction in the bottom panel.

3.2 Building the light curve

With $v(m)$, $X_{\rm Ni}(m)$, and $\kappa(m)$, we have everything we need to construct a light curve for each zone following Eq. (3). A zone is characterized by a unique peak time-scale,

$$t_{\rm pk}(m) \approx \left(\frac{m\kappa(m)}{4\pi c v(m)}\right)^{1/2}, \tag{8}$$

[2] A more physically motivated velocity profile can be derived from a power-law or exponential density profile $\rho(v)$ calibrated to simulations (e.g., Woosley et al. 2007). Here we choose the from of $v(m)$ in Eq. (5) since it can be expressed in a simple analytic form and gives decent qualitative agreement.

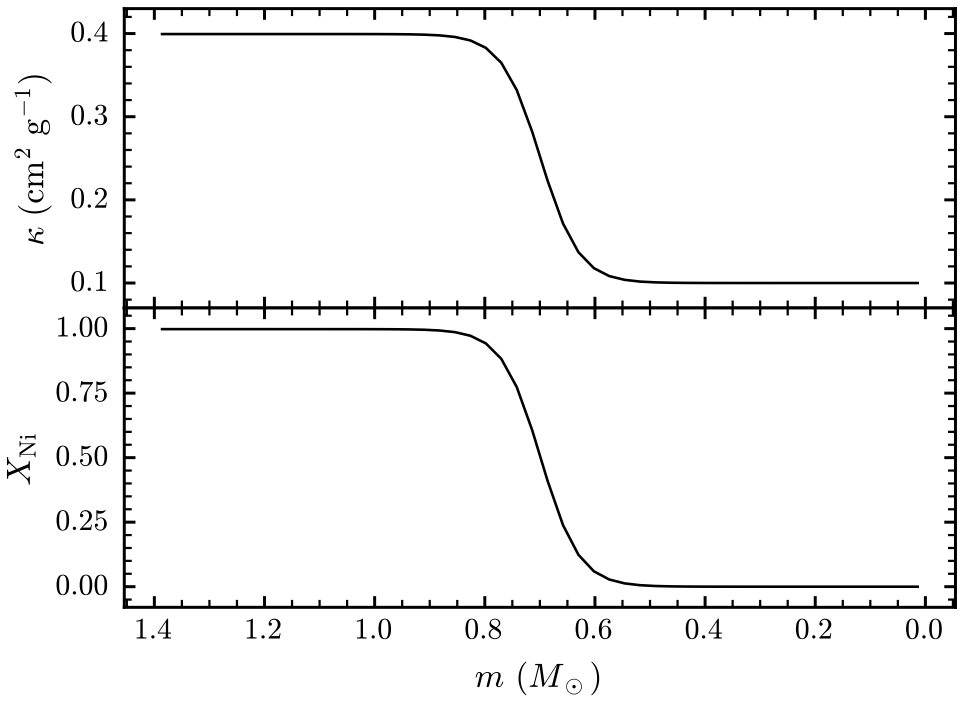

Figure 3:

Each zone will also have it's own heating function, depending on the amount of radioactive nickel in that zone $\dot{q}(m,t) = X_{\rm Ni}(m)\dot{q}(t)$. Then the total luminosity is obtained by integrating over all zones (Metzger et al., 2021),

$$L_{\rm tot}(t) = \frac{1}{M}\int_0^M L[t_{\rm pk}(m), \dot{q}(m,t), t]dm. \tag{9}$$

This is solved numerically for the parameters used in the ejecta model above; the results are presented in Fig. 4.

4 Suggested Exercises

1. What happens when you modify the total eject mass, velocity, opacity in the one-zone model? You can predict these effects using $t_{\rm pk} = \sqrt{M\kappa/4\pi vc}$. Vary the fiducial model parameters and see if the result matches expectations. What happens if you change the nickel mass?

2. Explore the effects of varying the above quantities and their profiles/distributions in the multi-zone model. You should feel free to explore unphysical extremes to see their exaggerated effects on the light curve.

3. **SN 2011fe**: Compare the model to the bolometric luminosity from SN 2011fe observations (Zhang et al., 2016). Use a linear time axis.

   (a) Adjust the total ^{56}Ni mass in the model to match the the peak luminosity from the data. How much nickel do you need?

   (b) You should find very food agreement between the early time morphology of the model light curve and the data. However, the model light curve overestimates the late time luminosity. Moreover, the slope of the late time emission in the model (which is the slope of the ^{56}Co decay heating) does not match the observed slope. Why do you think this is?

   (c) The late time emission slope in the data follows $f_{\rm th}(t)e^{-t/t_{\rm Co}}$. The extra factor is $f_{\rm th} \approx 1 - e^{-(t_\gamma/t)^2}$, where $t_\gamma \approx \sqrt{\kappa_\gamma M/4\pi v^2}$ is the time-scale for the ejecta to become optically thin to gamma rays.

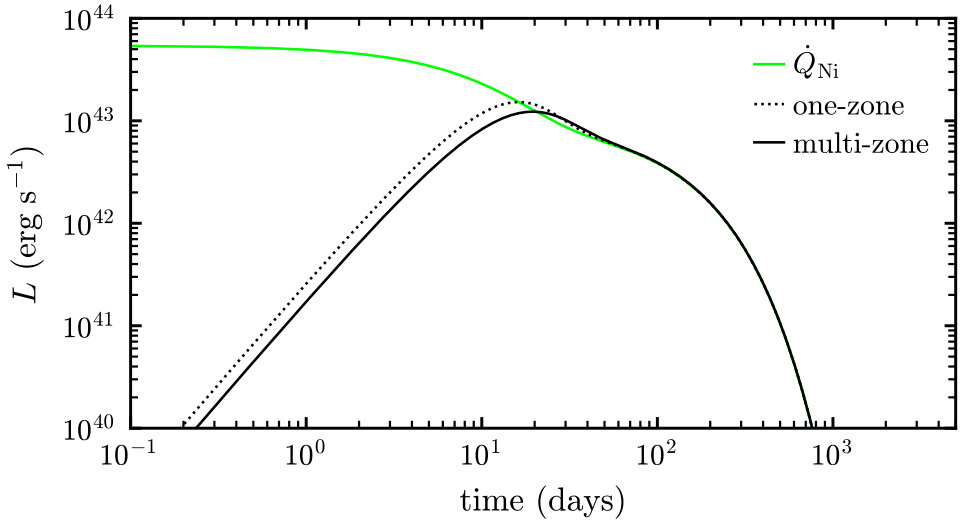

Figure 4: Multi-zone light curve model with parameters $M = 1.4M_\odot$, $M_{\rm Ni} = 0.7M_\odot$, $\bar{v} = 10000$ km s^{-1}, $f_{\rm mix} = 0.5$, $\kappa \approx 0.2$.

The opacity for ∼MeV gamma radiation is set primarily by Compton scattering, $\kappa_\gamma \approx 0.05$ cm^2 g^{-1} (Ambwani & Sutherland, 1988). Calculate t_γ for the model parameters and modify the original heating rate to account for gamma-ray thermalization, $\dot{q}_{\rm th}(t) = f_{\rm th}(t)\dot{q}(t)$. The new light curve slope should show better agreement with the data.

(d) Even with the appropriate light curve slope, you will find that the nickel mass inferred from fitting the peak luminosity (part a) over estimates the late-time luminosity. How much nickel mass do you need to fit the late-time emission? Do your two nickel mass estimates (from fitting the peak emission and from fitting the late-time emission) agree with the corresponding estimates from Zhang et al. (2016)? See Sec. 5.2 of Zhang et al. (2016) for a discussion of why the two methods might give different estimates of the nickel mass.

4. **Extra heating from ^{57}Ni**: Thus far we've assumed that ^{56}Ni is the only radioactive isotope synthesized in the explosion. In reality, other unstable iron group nuclei are synthesized and sometimes in significant amounts to affect the light curve. For example, it is known that ^{57}Ni can be synthesized in quantities at a few % of ^{56}Ni mass (Graur et al., 2016). The decay chain is ^{57}Ni $\rightarrow$^{57}Co $\rightarrow$^{57}Fe and the specific decay rate is given by Eq. 4, with $\epsilon_{\rm Ni} = 1.3 \times 10^{10}$ erg s^{-1} g^{-1}, $\epsilon_{\rm Co} = 6.1 \times 10^7$ erg s^{-1} g^{-1}, $t_{\rm Ni} = 2.1$ days, and $t_{\rm Co} = 392$ days. Note the long decay time-scale for ^{57}Co. How would you expect this to affect the light curve? Add $0.1M_\odot$ of ^{57}Ni to the explosion (in addition to the ^{56}Ni) and see if it matches your prediction.

5. ***r*-process doped SNe**: Modify the total ejecta mass, ^{56}Ni mass, and opacity to model a (hydrogen-poor) core-collapse supernova. It was originally believed that the neutrino driven wind following a successful core-collapse explosion would be an ideal site for the *r*-process (Meyer et al., 1992). Later studies discovered that these "ordinary" neutrino-driven CCSNe could not achieve the physical conditions required for the *r*-process (Qian & Woosley, 1996). However, an *r*-process may yet be possible in magneto-rotationally driven explosions (e.g., Mösta et al. 2018) or proto-magnetar winds (Prasanna et al., 2025). Collapsar disk winds may also have prolific *r*-process yields (Siegel et al., 2019). In all cases we would typically expect the *r*-process enriched ejecta to be embedded within the ordinary *r*-process-free supernova ejecta, so we can model the *r*-process distribution in the same way we handle the nickel mixing. The specific heating rate for *r*-process ejecta can be written as a power-law (Metzger et al., 2010),

$$\dot{q}_r = 3 \times 10^{10}\ {\rm erg\ s^{-1}\ g^{-1}} \left(\frac{t}{1\ {\rm day}}\right)^{-1.3}, \qquad (10)$$

and the typical continuum opacity is $1 - 30$ cm^2 g^{-1} (Tanaka et al., 2020), depending on the exact

composition of r-process nuclei. Add the heating function of Eq. (10) to the multi-zone model and assume $10^{-2} - 1 M_\odot$ of r-process material is synthesized (in addition to the ^{56}Ni!).

6. **Kilonovae**: There are two ejecta components with distinct properties (mass, velocity, and opacity) in neutron star mergers, producing the "blue" and "red" kilonova components (Kasen et al., 2017). The total bolometric kilonova light curve can be modeled by superimposing one-zone models for each component. Use the heating rate from the previous question and the ejecta properties from Kasen et al. (2017) to model a kilonova light curve.

References

Ambwani K., Sutherland P., 1988, ApJ, 325, 820

Arnett W. D., 1980, ApJ, 237, 541

Graur O., Zurek D., Shara M. M., Riess A. G., Seitenzahl I. R., Rest A., 2016, ApJ, 819, 31

Kasen D., Metzger B., Barnes J., Quataert E., Ramirez-Ruiz E., 2017, Nature, 551, 80

Metzger B. D., Martínez-Pinedo G., Darbha S., Quataert E., Arcones A., Kasen D., Thomas R., Nugent P., Panov I. V., Zinner N. T., 2010, MNRAS, 406, 2650

Metzger B. D., Zenati Y., Chomiuk L., Shen K. J., Strader J., 2021, ApJ, 923, 100

Meyer B. S., Mathews G. J., Howard W. M., Woosley S. E., Hoffman R. D., 1992, ApJ, 399, 656

Morozova V., Piro A. L., Renzo M., Ott C. D., Clausen D., Couch S. M., Ellis J., Roberts L. F., 2015, ApJ, 814, 63

Mösta P., Roberts L. F., Halevi G., Ott C. D., Lippuner J., Haas R., Schnetter E., 2018, ApJ, 864, 171

Patel A., Goldberg J. A., Renzo M., Metzger B. D., 2024, ApJ, 966, 212

Prasanna T., Coleman M. S. B., Thompson T. A., Metzger B. D., Patel A., Meyer B. S., 2025, arXiv e-prints, p. arXiv:2507.01094

Qian Y., Woosley S. E., 1996, ApJ, 471, 331

Siegel D. M., Barnes J., Metzger B. D., 2019, Nature, 569, 241

Tanaka M., Kato D., Gaigalas G., Kawaguchi K., 2020, MNRAS, 496, 1369

Woosley S. E., Kasen D., Blinnikov S., Sorokina E., 2007, ApJ, 662, 487

Zhang K., Wang X., Zhang J., Zhang T., Ganeshalingam M., Li W., Filippenko A. V., Zhao X., Zheng W., Bai J., Chen J., Chen J., Huang F., Mo J., Rui L., Song H., Sai H., Li W., Wang L., Wu C., 2016, ApJ, 820, 67